AUTOMATIC BOUNDARY INTEGRAL EQUATION PROGRAMS FOR THE PLANAR LAPLACE EQUATION

KENDALL ATKINSON* AND YOUNGMOK JEON†

Abstract. Algorithms with automatic error control are described for the solution of Laplace's equation on both interior and exterior regions, with both Dirichlet and Neumann boundary conditions. The algorithms are based on standard reformulations of each boundary value problem as a boundary integral equation of the second kind. The Nyström method is used to solve the integral equations, and convergence of arbitrary high order is observed when the boundary data is analytic. The Kelvin transformation is introduced to allow a simple conversion between internal and external problems. Two Fortran program implementations, DRCHLT and NEUMAN, are defined, analyzed, and illustrated.

Key words. Boundary integral equation, Laplace's equation, numerical integral equation, computer program

AMS subject classification. Primary: 65N38; Secondary 65R20, 45L10

1. Introduction. This paper presents two programs with automatic error control for solving Laplace's equation in two dimensions. The programs are based on solving standard boundary integral equation (BIE) reformulations of various boundary value problems. Let Ω denote a bounded simply connected planar region with a smooth boundary Γ. The programs treat both the Dirichlet and Neumann problems, for both interior and exterior regions, for such regions Ω.

We use standard BIE reformulations of Laplace's equation, and the numerical methods are also quite standard. The programs are of interest in that they are automatic in selecting various problem parameters so as to ensure a requested error tolerance. Moreover, we believe the programs are robust and relatively efficient, especially when the requested error tolerances are small or when the region Ω is not convex and has a complicated boundary. The NAG library [8] contains a routine *D03EAF* for using boundary integral representations to solve Laplace's equation. That program requires the user to specify the discretization parameter, and it does not contain any means to estimate the error in the computed solution, in contrast to our codes. For that reason, we have not included any numerical comparisons with *D03EAF*. Our codes, however, are restricted to smooth boundaries Γ, which is not a restriction with the NAG routine.

In §2, we review the reformulation of the interior Dirichlet problem and the exterior Neumann problems as boundary integral equations; and we describe the numerical method used to solve these BIE. In §3, this work is extended to the exterior Dirichlet and interior Neumann problems, by means of applying a Kelvin transformation to convert the problems to those treated in §2. In §4, we describe the algorithms DRCHLT for the solution of the Dirichlet problem and NEUMAN for the Neumann problem. Numerical examples which explore the behaviour of the algorithms are given in §5. We note

* Dept of Mathematics, University of Iowa, Iowa City, IA 52242. This research is supported in part by NSF grant DMS-9403589

† Dept of Mathematics, A-Jou University, Su Won, Korea 441-749. The research is supported by Korean Ministry of Education under the grant number BSRI-96-1441.

particularly the numerical example for the "amoeba" boundary of Figure 2, as it is a region which would give a great deal of trouble to finite element and finite difference codes.

2. The Interior Dirichlet and Exterior Neumann Problems. The material of this and the following section is well-known, and the reader can find an extensive development of it in [4, Chap. 7], Kress [5], or in a number of other texts on boundary integral equations. Consider first the interior Dirichlet problem

$$\begin{aligned} \Delta u(A) &= 0, \qquad A \in \Omega \\ u(P) &= f(P), \quad P \in \Gamma \end{aligned} \tag{1}$$

and assume that Γ has a parameterization which is at least twice continuously differentiable. Represent u as a double layer potential

$$u(A) = -\int_\Gamma \rho(Q) \frac{\partial}{\partial n_Q} \left[\log |A-Q|\right] dS_Q, \quad A \in \Omega \tag{2}$$

in which n_Q is the outward unit normal at $Q \in \Gamma$. Then ρ satisfies the uniquely solvable integral equation

$$-\pi\rho(P) - \int_\Gamma \rho(Q) \frac{\partial}{\partial n_Q} \left[\log |P-Q|\right] dS_Q = f(P), \quad P \in \Gamma \tag{3}$$

Parameterize Γ by $\mathbf{r}(t) = (x(t), y(t))$, $0 \le t \le 2\pi$, where we assume $|\mathbf{r}'(t)| \neq 0$ for all t. Rewrite (3) as

$$-\pi\rho(t) - \int_0^{2\pi} \rho(s) K(t,s)\, ds = f(t), \quad 0 \le t \le 2\pi \tag{4}$$

In this, we have identified $\rho(\mathbf{r}(t))$ with $\rho(t)$, for simplicity. For the kernel function,

$$K(t,s) = \begin{cases} \dfrac{y'(s)\left[x(s)-x(t)\right] - x'(s)\left[y(s)-y(t)\right]}{\left[x(s)-x(t)\right]^2 + \left[y(s)-y(t)\right]^2}, & t \neq s \\ \dfrac{y''(t)x'(t) - x''(t)y'(t)}{2\left[x'(t)^2 + y'(t)^2\right]}, & t = s \end{cases} \tag{5}$$

With the assumption that $\mathbf{r}(t)$ is at least twice continuously differentiable, the kernel function $K(t,s)$ is continuous; and for $\mathbf{r} \in C^{q+2}$, it follows that $K \in C^q$ with respect to all partial derivatives of K. We write (4) symbolically as

$$(-\pi - \mathcal{K})\,\rho = f$$

The most efficient way to solve (4) is to use the Nyström method with the rectangle rule. This is because the integral in (4) is periodic in s with period 2π, and for such cases, the rectangle rule (or equivalently the trapezoidal rule, due to periodicity) is

a very rapidly convergent method. For example, if g belongs to the Sobolev space $H^\beta[0,2\pi]$ for some $\beta > \frac{1}{2}$, and if g is periodic on $[0,2\pi]$, then

$$\left| \int_0^{2\pi} g(s)\,ds - h\sum_{j=1}^{n} g\,(s_j) \right| \leq \frac{\sqrt{4\pi\zeta(2\beta)}}{n^\beta}\,\|g\|_{H^\beta}\,, \quad n \geq 1 \tag{6}$$

with $h = 2\pi/n$, $s_j = jh$ for $j = 1, ..., n$, and $\zeta(t)$ the Riemann Zeta function.

The Nyström approximation of (4) is given by

$$-\pi\rho_n(t) - h\sum_{j=1}^{n} K(t,s_j)\rho_n(s_j) = f(t), \quad 0 \leq t \leq 2\pi \tag{7}$$

We write this symbolically as

$$(-\pi - \mathcal{K}_n)\,\rho_n = f$$

with the numerical integral operator $\mathcal{K}_n$ defined implicitly by (7). The equation (7) is equivalent in solvability to the linear system

$$-\pi\rho_n(s_i) - h\sum_{j=1}^{n} K(s_i,s_j)\rho_n(s_j) = f(s_i), \quad i = 1, ..., n \tag{8}$$

The equivalence of these two formulas is given by the *Nyström interpolation formula*

$$\rho_n(t) = -\frac{1}{\pi}\left[f(t) + h\sum_{j=1}^{n} K(t,s_j)\rho_n(s_j) \right], \quad 0 \leq t \leq 2\pi \tag{9}$$

enabling one to extend the solution $\{\rho_n(s_i)\}$ of (8) to $\rho_n(s)$ for general s. The equivalence is discussed in [4, p. 101]. We write (8) symbolically as

$$(-\pi - K_n)\,\boldsymbol{\rho}_n = \mathbf{f}_n, \qquad \boldsymbol{\rho}_n, \mathbf{f}_n \in \mathbb{R}^n \tag{10}$$

By standard error analysis results (e.g. see [4, Chap. 4]), the operators $-\pi - \mathcal{K}_n$ are invertible for all sufficiently large n, say $n \geq n_0$, and their inverses are uniformly bounded. Moreover,

$$\|\rho - \rho_n\|_\infty \leq \left\|(-\pi - \mathcal{K}_n)^{-1}\right\| \|\mathcal{K}\rho - \mathcal{K}_n\rho\|_\infty\,, \quad n \geq n_0 \tag{11}$$

Thus the smoother the curve and the smoother the data f, the faster the uniform convergence of ρ_n to ρ. Precise bounds can be obtained from either (6) or the Euler-MacLaurin formula (cf. [3, p. 285]). Using the latter, we have the following result. Let Γ be $(q+2)$-times differentiable, let $\rho \in C^p(\Gamma)$, and let $r = \min\{p, q\}$. Then

$$\|\rho - \rho_n\|_\infty \leq \frac{c}{n^r}\left\|\rho^{(r)}\right\|_\infty \tag{12}$$

for some c independent of n and r. By differentiating the equations (4) and (7) with respect to t, we can also obtain bounds on the rate of convergence of $\rho_n^{(k)}$ to $\rho^{(k)}$:

$$\left\|\rho^{(k)} - \rho_n^{(k)}\right\|_\infty \leq \frac{c_{r,k}}{n^{r-k}} \left\|\rho^{(r)}\right\|_\infty, \qquad k = 1, ..., r-1$$

for some $c_{r,k}$ independent of n.

To solve approximately the Dirichlet problem (1), introduce the approximating potential

$$u_n(A) = -\int_\Gamma \rho_n(Q) \frac{\partial}{\partial n_Q} \left[\log |A - Q|\right] dS_Q, \quad A \in \Omega \tag{13}$$

Using the parameterization of Γ, rewrite this as

$$u_n(A) = -\int_0^{2\pi} \rho_n(s) K_A(s)\, ds, \quad A \in \Omega \tag{14}$$

$$K_A(s) = |\mathbf{r}'(s)| \left.\frac{\partial}{\partial n_Q} \left[\log |A - Q|\right]\right|_{Q=\mathbf{r}(s)}$$

The function u_n is harmonic on Ω. To look at the error $u - u_n$, note first that by the maximum principle,

$$|u(A) - u_n(A)| \leq \max_{P \in \Gamma} |u(P) - u_n(P)| \tag{15}$$

Let $A \to P \in \Gamma$ in (13) and then subtract from (3) to obtain

$$-\pi \left[\rho(P) - \rho_n(P)\right] - \int_\Gamma \left[\rho(Q) - \rho_n(Q)\right] \frac{\partial}{\partial n_Q} \left[\log |P - Q|\right] dS_Q = u(P) - u_n(P), \quad P \in \Gamma$$

Then

$$\max_{P \in \Gamma} |u(P) - u_n(P)| \leq (\pi + \|\mathcal{K}\|) \left\|\rho - \rho_n\right\|_\infty$$

When combined with (15),

$$|u(A) - u_n(A)| \leq (\pi + \|\mathcal{K}\|) \left\|\rho - \rho_n\right\|_\infty, \quad A \in \Omega \tag{16}$$

If the region Ω is convex, then $\|\mathcal{K}\| = \pi$ and the bound simplifies further. In the program, we use the approximation

$$\|\mathcal{K}\| = \max_t \int_0^{2\pi} |K(t,s)|\, ds \doteq h \max_{1 \leq i \leq n} \sum_{j=1}^{n} |K(s_i, s_j)|$$

It is not difficult to see that $K_A(s)$ is very peaked for A near to Γ, with the maximum peaking occurring at the point of Γ nearest to A. For that reason, we use a standard integral identity to write

$$u_n(A) = -2\pi\rho_n(s^*) - \int_0^{2\pi} [\rho_n(s) - \rho_n(s^*)]\, K_A(s)\, ds, \quad A \in \Omega \tag{17}$$

with s^* chosen to approximately minimize $|\mathbf{r}(s) - A|$. This new integral is slightly better in terms of its behaviour for s near to s^*. This is a standard technique, long used to reduce the effect of the peak in $K_A(s)$.

To evaluate (17), we again use the rectangle rule, say with m nodes:

$$u_{n,m}(A) = -2\pi\rho_n(s^*) - \eta \sum_{j=1}^{m} [\rho_n(\sigma_j) - \rho_n(s^*)]\, K_A(\sigma_j) \tag{18}$$

with $\eta = 2\pi/m$, $\sigma_j = j\eta$, $j = 1, 2, ..., m$. In our program, we begin with $n = n_0 = 16$, doubling as needed. The values of m begin with $m = m_0 = 32$; and m is doubled as needed. When m exceeds n, the Nyström formula (9) is used to extend ρ_n to new argument values; and these are saved for possible use with other points A. The size of m is limited by the size of the workspace given to the subroutine DRCHLT.

For the total error in $u_{n,m}(A)$,

$$\begin{aligned} |u(A) - u_{n,m}(A)| &\le |u(A) - u_n(A)| + |u_n(A) - u_{n,m}(A)| \\ &= \left\{ \frac{c}{n^r} (\pi + \|\mathcal{K}\|) + \frac{c'}{\delta^r m^r} \right\} \left\| \rho^{(r)} \right\|_\infty \end{aligned} \tag{19}$$

In this, the bound on $|u_n(A) - u_{n,m}(A)|$ comes from [6], with

$$\delta = \min_{P \in \Gamma} |A - P|$$

The power of δ in the denominator would be one greater if (13) had been used rather than (17).

2.1. The exterior Neumann problem. Consider the exterior Neumann problem

$$\begin{aligned} \Delta u(A) &= 0, & A \in \Omega_e \\ \frac{\partial u(P)}{\partial n_P} &= g(P), & P \in \Gamma \\ u(A) &\to 0 & \text{as } |A| \to \infty \end{aligned} \tag{20}$$

in which $\Omega_e = \mathbb{R}^2 / \overline{\Omega}$. Again, n_P is directed into Ω_e. Note that in the exterior Neumann problem,

$$u(A) \to 0 \text{ as } |A| \to \infty \quad \Leftrightarrow \quad \int_\Gamma \frac{\partial u(P)}{\partial n_P} dS_P = \int_\Gamma g(P) dS_P = 0 \tag{21}$$

For details, see Kress [5].

Represent the solution u of (20) as a single layer potential,

$$u(A) = -\int_\Gamma \psi(Q) \log|A-Q|\, dS_Q, \quad A \in \Omega_e \tag{22}$$

By standard arguments, ψ satisfies the equation

$$-\pi\psi(P) - \int_\Gamma \psi(Q) \frac{\partial}{\partial n_P} [\log|P-Q|]\, dS_Q = g(P), \quad P \in \Gamma \tag{23}$$

Using the parameterization $\mathbf{r}(t) = (x(t), y(t))$ for Γ, (23) becomes

$$-\pi\psi(t) - \int_0^{2\pi} \psi(s) K_e(t,s)\, ds = g(t), \quad 0 \le t \le 2\pi \tag{24}$$

For the kernel function,

$$K_e(t,s) = \begin{cases} \dfrac{y'(t)\,[x(s)-x(t)] - x'(t)\,[y(s)-y(t)]}{[x(s)-x(t)]^2 + [y(s)-y(t)]^2} \cdot \dfrac{\sqrt{x'(s)^2+y'(s)^2}}{\sqrt{x'(t)^2+y'(t)^2}}, & t \ne s \\ \dfrac{y''(t)x'(t) - x''(t)y'(t)}{2\,[x'(t)^2+y'(t)^2]}, & t = s \end{cases}$$

The integral equation (24) is solved in the same manner as earlier with the interior Dirichlet problem, resulting in an approximation ψ_n; and the error bounds and rates of convergence are also as before. For the approximation of u, introduce

$$u_n(A) = -\int_\Gamma \psi_n(Q) \log|A-Q|\, dS_Q, \quad A \in \Omega_e \tag{25}$$

Using the parameterization of Γ, we write

$$u_n(A) = -\int_0^{2\pi} \psi_n(s) K_{e,A}(s)\, ds, \quad A \in \Omega_e \tag{26}$$

$$K_{e,A}(s) = |\mathbf{r}'(s)| \log|A - \mathbf{r}(s)|$$

Using the maximum principle and arguing as before,

$$|u(A) - u_n(A)| \le \|\psi - \psi_n\|_\infty \sup_{P\in\Gamma} \int_\Gamma |\log|P-Q||\, dS_Q, \quad A \in \Omega_e \tag{27}$$

We approximate $u_n(A)$ by $u_{n,m}(A)$, much as before in (18):

$$u_{n,m}(A) = -\eta \sum_{j=1}^{m} \psi_n(\sigma_j) K_{e,A}(\sigma_j), \quad A \in \Omega_e \tag{28}$$

The error bound for $|u(A) - u_{n,m}(A)|$ is exactly the same as that in (19) for the approximation of the double layer potential, with ρ replace by ψ and with other choices for c and c'.

For the case that $P \in \Gamma$, we must use an alternative to (28). Rewrite (26) as

$$u_n(\mathbf{r}(t)) = \pi \mathcal{A}\widetilde{\psi}_n(t) - \mathcal{R}\widetilde{\psi}_n(t), \qquad 0 \le t \le 2\pi \tag{29}$$

In this, we write $\widetilde{\psi}_n(t) = \psi_n(t)\,|\mathbf{r}'(t)|$,

$$\mathcal{A}\varphi(t) \equiv -\frac{1}{\pi}\int_0^{2\pi} \log\left|2e^{-\frac{1}{2}}\sin\left(\frac{t-s}{2}\right)\right| \varphi(s)\,ds$$

$$\mathcal{R}\varphi(t) \equiv \int_0^{2\pi} \log\left|\frac{\mathbf{r}(t)-\mathbf{r}(s)}{2e^{-\frac{1}{2}}\sin\left(\frac{t-s}{2}\right)}\right| \varphi(s)\,ds \equiv \int_0^{2\pi} R(t,s)\varphi(s)\,ds$$

It is well-known that $\mathcal{A} : H^p(0,2\pi) \xrightarrow[onto]{1-1} H^{p+1}(0,2\pi)$ for these Sobolev spaces, with $p \ge 0$. Moreover,

$$\mathcal{A}\left(\sum_{k=-\infty}^{\infty} a_k e^{ikt}\right) = \sum_{k=-\infty}^{\infty} \frac{a_k}{k^*} e^{ikt}, \quad k^* \equiv \max\{1, |k|\} \tag{30}$$

Also, the kernel of $\mathcal{R}$ is smooth; and for $\mathbf{r} \in C^{q+1}$, the kernel is in C^q, $q \ge 0$, with respect to both s and t. We combine these results to give an accurate means of numerically approximating u_n in (29).

Let l be an even integer, and let $\tau_j = 2\pi j/l,\ j = 1, ..., l$. Let $\widetilde{\psi}_{n,l}(t)$ be the Fourier approximation of degree $l/2$ for $\widetilde{\psi}_n(t)$ given by

$$\widetilde{\psi}_{n,l}(t) = \sum_{k=-l/2}^{l/2} a_k^{(n,l)} e^{ikt}, \qquad a_k^{(n,l)} = \frac{1}{l}\sum_{j=1}^{l} \widetilde{\psi}_n(\tau_j) e^{-ik\tau_j} \tag{31}$$

Then we approximate $u_n(\mathbf{r}(t))$ by

$$u_{n,l,m}(\mathbf{r}(t)) = \pi \mathcal{A}\widetilde{\psi}_{n,l}(t) - \mathcal{R}_m\widetilde{\psi}_n(t) \tag{32}$$

$$\mathcal{R}_m\widetilde{\psi}_n(t) = \eta \sum_{j=1}^{m} \widetilde{\psi}_n(\sigma_j) R(t, \sigma_j)$$

recalling the definitions of η and $\{\sigma_j\}$ from (18). The term $\mathcal{A}\widetilde{\psi}_{n,l}(t)$ is calculated from (30).

As in the analysis of the error for the Dirichlet problem, assume $\mathbf{r} \in C^{q+2}$ and $g \in C^p$, and let $r = \min\{p, q\}$. For the error in $\widetilde{\psi}_{n,l}(t)$,

$$\begin{aligned} \left\| \widetilde{\psi} - \widetilde{\psi}_{n,l} \right\|_\infty &\leq \left\| \widetilde{\psi} - \widetilde{\psi}_n \right\|_\infty + \left\| \widetilde{\psi}_n - \widetilde{\psi}_{n,l} \right\|_\infty \\ &\leq \frac{c_1}{n^r} \left\| \widetilde{\psi}^{(r)} \right\|_\infty + \frac{c_2 \log l}{l^r} \left\| \widetilde{\psi}_n^{(r)} \right\|_\infty \end{aligned}$$

with the Fourier approximation error bound based on standard results (e.g. see [3, p. 180]). Also,

$$\begin{aligned} \left\| \mathcal{R}\widetilde{\psi} - \mathcal{R}_m \widetilde{\psi}_n \right\|_\infty &\leq \left\| \mathcal{R}\widetilde{\psi} - \mathcal{R}\widetilde{\psi}_n \right\|_\infty + \left\| \mathcal{R}\widetilde{\psi}_n - \mathcal{R}_m \widetilde{\psi}_n \right\|_\infty \\ &\leq \frac{c_3}{n^r} \left\| \widetilde{\psi}^{(r)} \right\|_\infty + \frac{c_4}{m^r} \left\| \widetilde{\psi}_n^{(r)} \right\|_\infty \end{aligned}$$

Returning to the analysis of the Nyström method, it is straightforward to show that

$$\left\| \widetilde{\psi}_n^{(r)} \right\|_\infty \leq c_5 \left\| \widetilde{\psi}^{(r)} \right\|_\infty$$

and we omit the proof. Combining these results, we have

$$\begin{aligned} \left\| u\left(\mathbf{r}(\cdot)\right) - u_{n,l,m}\left(\mathbf{r}(\cdot)\right) \right\|_\infty &\leq \pi \left\| \mathcal{A}\widetilde{\psi} - \mathcal{A}\widetilde{\psi}_{n,l} \right\|_\infty + \left\| \mathcal{R}\widetilde{\psi} - \mathcal{R}_m \widetilde{\psi}_n \right\|_\infty \\ &\leq \left\{ \frac{c_6}{n^r} + \frac{c_7 \log l}{l^r} + \frac{c_8}{m^r} \right\} \left\| \widetilde{\psi}^{(r)} \right\|_\infty \end{aligned} \tag{33}$$

For smooth curves Γ and smooth data g, the covergence will be quite rapid. The coefficients $\left\{ a_k^{(n,l)} \right\}$ can be evaluated quite rapidly with a FFT, which we have incorporated into our code. The routine used is DRFFT from Swarztrauber [10] with a minor modification.

The above approximations for solving (20) are incorporated into the program NEUMAN. This and DRCHLT are discussed in §4, including a description the error prediction mechanisms.

3. The Exterior Dirichlet and Interior Neumann Problems. We begin by introducing the Kelvin transformation, and we use it to reformulate the exterior Dirichlet and interior Neumann problems as interior Dirichlet and exterior Neumann problems, respectively. Define $\mathcal{T} : \mathbb{R}^2/\{(0,0)\} \to \mathbb{R}^2/\{(0,0)\}$ by

$$\mathcal{T}(x, y) = (\widetilde{x}, \widetilde{y}) = \left(\frac{x}{r^2}, \frac{y}{r^2} \right), \qquad r^2 = x^2 + y^2 \tag{34}$$

Also introduce $\widetilde{r}^2 = \widetilde{x}^2 + \widetilde{y}^2$, and note that $r\widetilde{r} = 1$. In addition, define the Kelvin transformation of a function u by

$$\widetilde{u}(\widetilde{x}, \widetilde{y}) = u(x, y), \qquad (\widetilde{x}, \widetilde{y}) = \mathcal{T}(x, y) \tag{35}$$

Assume Ω contains the origin $(0,0)$, and define

$$\widetilde{\Omega} = \{(\widetilde{x},\widetilde{y}) = \mathcal{T}(x,y) \mid (x,y) \in \Omega\}$$

and $\widetilde{\Gamma}$ is the boundary of $\widetilde{\Omega}$.

Introduce the exterior Dirichlet problem:

$$\begin{aligned} \Delta u(A) &= 0, & A &\in \Omega_e \\ u(P) &= f(P), & P &\in \Gamma \\ u(A) &\to C & &\text{as } |A| \to \infty \end{aligned} \tag{36}$$

with C a given constant. Also introduce the interior Neumann problem

$$\begin{aligned} \Delta u(A) &= 0, & A &\in \Omega \\ \frac{\partial u(P)}{\partial n_P} &= g(P), & P &\in \Gamma \\ u(0,0) &= 0 \end{aligned} \tag{37}$$

As is well-known, this has a unique solution provided that

$$\int_\Gamma g(Q)\, dS_Q = 0 \tag{38}$$

All solutions without the restriction $u(0,0) = 0$ are obtained by merely adding an arbitrary constant to the given solution u of (37). We reformulate these boundary value problems using (35).

The exterior problem (36) is equivalent to the following interior problem: find $\widetilde{u}$ such that

$$\begin{aligned} \Delta\widetilde{u}(\widetilde{A}) &= 0, & \widetilde{A} &\in \widetilde{\Omega}_e \\ \widetilde{u}(\widetilde{P}) &= f(\mathcal{T}^{-1}\widetilde{P}), & \widetilde{P} &\in \widetilde{\Gamma} \\ \widetilde{u}(0,0) &= C \end{aligned} \tag{39}$$

The interior Neumann problem (37) is equivalent to the following exterior problem: find $\widetilde{u}$ such that

$$\begin{aligned} \Delta\widetilde{u}(\widetilde{A}) &= 0, & \widetilde{A} &\in \Omega \\ \frac{\partial\widetilde{u}(\widetilde{P})}{\partial n_{\widetilde{P}}} &= -\frac{1}{\widetilde{r}^2} g(\mathcal{T}^{-1}\widetilde{P}), & \widetilde{P} &\in \Gamma \\ \widetilde{u}(\widetilde{A}) &\to 0 & &\text{as } \left|\widetilde{A}\right| \to \infty \end{aligned} \tag{40}$$

The proofs are omitted as this is standard material; see [4, §7.1].

We can now solve the problems (36) and (37) by applying the methods of the preceding section. This reformulation process is incorporated into the codes DRCHLT and NEUMAN.

4. Numerical Algorithms. Many of the ideas are the same for both DRCHLT and NEUMAN, and we choose to introduce them for only DRCHLT. Later in the section, we discuss the differences which occur in NEUMAN. We also discuss the problems (1) and (20) of §2, as those in §3 follow easily by applying the Kelvin transformation. The programs are written in double precision in *Fortran 77*, but are compatible with *Fortran 90*.

In DRCHLT, we first call INTEQN to generate the density function ρ_n of (7); and we call EVALU to evaluate $u_{n,m}$ from (18). Summary outlines of INTEQN and EVALU are given later in §4.1. In INTEQN, we set up and solve the linear system (8), using LAPACK routines [1] for the Gaussian elimination. We could have used an iterative technique to solve the linear system, but the systems being used are of such size that it is both simpler and equally fast to just use a direct method of solution.

The stopping criteria for INTEQN for the current values of n and ρ_n is based on the estimate

$$EST \equiv \text{cond}(\pi + K_n)\,(\pi + \|\mathcal{K}\|)\,\frac{\lambda}{1-\lambda}\left\|\rho_n - \rho_{\frac{1}{2}n}\right\|_\infty \tag{41}$$

for the right side of the error bound (16). This bound is obtained as follows. In (16), we estimate $\|\rho - \rho_n\|_\infty$ using

$$\|\rho - \rho_n\|_\infty \doteq \frac{\lambda}{1-\lambda}\left\|\rho_n - \rho_{\frac{1}{2}n}\right\|_\infty \tag{42}$$

and

$$\left\|\rho_n - \rho_{\frac{1}{2}n}\right\|_\infty \doteq \max_{j=1,\ldots,\frac{1}{2}n}\left|\rho_n(jh_o) - \rho_{\frac{1}{2}n}(jh_o)\right|, \quad h_o = \frac{2\pi}{\frac{1}{2}n}$$

The constant $\lambda < 1$ is meant to estimate the rate of convergence of ρ_n to ρ. In the program, we have both a conservative and a normal way to define this rate λ (denoted by $RATE$ in INTEQN). The normal way of defining it is by

$$\lambda = \frac{\left\|\rho_n - \rho_{\frac{1}{2}n}\right\|_\infty}{\left\|\rho_{\frac{1}{2}n} - \rho_{\frac{1}{4}n}\right\|_\infty} \tag{43}$$

with λ restricted to lay in the interval $[RTLOW, RTUP]$. These limits are defined in an introductory DATA statement in INTEQN by

$$[RTLOW, RTUP] = [0.1, 0.5]$$

For the initial two choices of n in our program INTEQN, we always use $\lambda = RTUP$. The choice (43) is a fairly conservative choice, since (12) implies that the true rate λ should tend to zero as $n \to \infty$. The more conservative way of defining λ in our program is by choosing

$$RATE = RTUP \tag{44}$$

and this choice leads to the error estimate

$$EST \equiv \text{cond}(A_n)\,(\pi + \|\mathcal{K}\|)\left\|\rho_n - \rho_{\frac{1}{2}n}\right\|_\infty$$

The first estimate (43) usually results in less computation, and the value of $RTLOW$ could even be made smaller for quite well-conditioned problems. For fairly ill-conditioned problems with an error tolerance ε that is fairly large, say $\varepsilon \approx 10^{-2}$ to 10^{-4}, it is probably better to use the conservative choice of λ in (44), as the asymptotic estimate (42) is less likely to be accurate in this situation.

In (41), we have included the term $\text{cond}(\pi + K_n)$, multiplying the right side of (16), to take into account changes in the solution due to the conditioning of the linear system of (10).

We accept ρ_n as being sufficiently accurate if the test

$$EST \le \frac{\varepsilon}{2} \tag{45}$$

is satisfied, where ε is a given error tolerance for the solution u of the boundary value problem (1). If this test is satisfied, then (16) is likely to be satisfied with

$$\max|u(A) - u_n(A)| \le EST \le \frac{\varepsilon}{2}, \qquad A \in \Omega \tag{46}$$

We must then evaluate $u_{n,m}(A)$ with sufficient accuracy for each given A.

Given $A \in \Omega$, we use EVALU to calculate $u_{n,m}(A)$ from (18) with m so chosen that

$$|u_n(A) - u_{n,m}(A)| \le \frac{\varepsilon}{2} \tag{47}$$

To do this, we must first find the point s^* of (17)-(18) which approximately minimizes $|A - \mathbf{r}(s)|$. Initially we use a simple check of the node points s at which $\rho_n(s)$ has already been computed. In general, we accept a point $s = s^*$ as acceptable if

$$|\cos\theta| \le .01 \tag{48}$$

for the angle θ between $\mathbf{r}(s^*) - A$ and the tangent vector $\mathbf{r}'(s^*)$. As the point A approaches the boundary Γ, this simple procedure is not adequate and we must use a rootfinding method to calculate s^*. We use Newton's method if it appears to be converging, and otherwise we use the bisection method.

In the evaluation of $u_{n,m}(A)$, m is doubled repeatedly until $u_{n,m}(A)$ satisfies (47), and our codes begin with $m = 32$. We use an estimate of $|u_n(A) - u_{n,m}(A)|$ to decide on an acceptable value of m. When $m > n$, we evaluate $\rho_n(\sigma_i)$ at new node points $\{\sigma_i\}$ using the Nyström interpolation formula (9); and such values are stored for later use with other evaluations of u_n. The basic stopping criteria in EVALU for accepting $u_{n,m}(A)$ is the test

$$|u_n(A) - u_{n,m}(A)| \doteq \frac{\mu}{1-\mu}\left|u_{n,m}(A) - u_{n,\frac{1}{2}m}(A)\right| \le \frac{\varepsilon}{2} \tag{49}$$

As in INTEQN, there are two choices for μ (which is called $RATE$ within EVALU). The normal choice is to define μ by

$$\mu = \frac{\left| u_{n,m}(A) - u_{n,\frac{1}{2}m}(A) \right|}{\left| u_{n,\frac{1}{2}m}(A) - u_{n,\frac{1}{4}m}(A) \right|} \tag{50}$$

This is also restricted to lay in an interval

$$[RTLOW, RTUP] = [0.1, 0.5]$$

so as to be neither too large nor too small. The conservative choice for μ is again to use

$$\mu = RTUP \tag{51}$$

Again, this seems necessary for more ill-conditioned problems.

The maximum allowable size for m is determined from the size of the work space vector supplied by the user to DRCHLT. The introductory comments for DRCHLT contain detailed information on the parameters to be supplied to the routine, and we omit those here.

For NEUMAN, we use the same framework as described above. The error test for accepting ψ_n must be modified in consonance with (27), but that is straightforward and we omit it here. When evaluating $u_n(P)$ for $P \in \Gamma$, we approximate ψ_n using a Fourier approximation, as is described in §2.1 following (31). The needed value of l is determined experimentally by comparing the approximations of ψ_n for parameters l and $2l$. The Fourier coefficients of (31) are evaluated with an FFT program of Swarztrauber [10].

4.1. An outline of the codes. The routine DRCHLT coordinates the use of INTEQN and EVALU, including dividing up the working storage delivered to DRCHLT by the user. It first calls the subroutine INTEQN, which has the following approximate outline.

1. Initialize for a loop on n, the number of nodes.
2. Do steps 3 through 7 until the error test in step 7 is satisfied.
3. Calculate the boundary nodal points on Γ for n subdivisions.
4. Set up the linear system (8) and estimate $\|\mathcal{K}\|$.
5. Solve the linear system (8) for $\{\rho_n(s_i) \mid i = 1, ..., n\}$.
6. Update the value of $RATE$ and EST.
7. If $EST \leq \varepsilon/2$, then return to DRCHLT.

The program EVALU has the following approximate outline.

1. Initialize for a loop on the number of given points A at which $u(A)$ is to be approximated.
2. For point A_i, do steps 3 through 9 until the error test in step (47) is satisfied.
3. Initialization of variables for integration of $u_n(A_i)$.

4. Calculate s^*. Begin by consideration of points s at which $\rho_n(s)$ is already known. If (48) is satisfied go to next step. Otherwise, solve for s^* using Newton's method or the bisection method.
5. Begin numerical integration (18) with $m = m_0/2$ nodes.
6. Loop thru step 8 on m, beginning with $m = m_0$ nodes. Compare the results for m and $\frac{1}{2}m$ nodes, updating μ in (50) as needed.
7. Calculate error estimate (49) for numerical integration error.
8. If integration error estimate satisfies (47), then end integration.
9. Calculate an error estimate for the approximation $u_{n,m}(A_i)$, and then go to the consideration of the next point A_i.

In both INTEQN and EVALU, the storage limitations are checked at all stages; and when these restrict obtaining the desired accuracy, appropriate error indicators are set. The program NEUMAN is organized similarly to the above, except for the inclusion of the option of computing the solution $u(A)$ at points $A \in \Gamma$, using the procedure described following (29).

4.2. Computational complexity. What is the computational cost of using DRCHLT or NEUMAN? The cost of solving a single linear system of order k by Gaussian elimination is well-known to be approximately $\frac{2}{3}k^3$ arithmetic operations. If we solve systems of orders

$$k = n_0, 2n_0, ..., n_f \tag{52}$$

(with $n_0 = 16$ in our code), then the total cost for the solution of linear systems is approximately

$$\frac{2}{3}\left(n_0^3 + 8n_0^3 + \cdots + 8^\nu n_0^3\right) = \frac{2}{21}\left(8^{\nu+1} - 1\right) n_0^3, \qquad \nu = \log_2\left(\frac{n_f}{n_0}\right) \tag{53}$$

We have not found it necessary to go above $\nu = 5$ in the vast majority of our examples because of the rapid convergence of the trapezoidal numerical integration of (7). The value of n_0 can be changed by simply changing the variable N_0 in the DATA statement of INTEQN. The cost of setting up the coefficient matrix of (10), $-\pi I - K_n$, is n^2 evaluations of the kernel function $K(t,s)$ of (5); and the total cost for the indices of (52) is

$$\frac{2}{9}\left(4^{\nu+1} - 1\right) n_0^2$$

evaluations of $K(t,s)$.

The cost of evaluating $u_{n,m}(A)$ using the trapezoidal rule in (18) for the indices

$$m = \ell_0, ..., \ell_f$$

is

$$\ell_0 + 2\ell_0 + \cdots + 2^\gamma \ell_0 = \left(2^{\gamma+1} - 1\right)\ell_0, \qquad \gamma = \log_2\left(\frac{\ell_f}{\ell_0}\right) \tag{54}$$

arithmetic operations for the sum and the same number of evaluations of the kernel function $K_A(s)$. In our program, $\ell_0 = 16$; and it can be reset by changing the variable $M\_0 \equiv 2\ell_0$ in the DATA statement of EVALU. If the approximate solution $u_{n,m}(A)$ is to be evaluated at a very large number of points A, then this can be an expensive proposition, especially if some of the points A are close to the boundary Γ. Again, however, the trapezpoidal rule converges very rapidly if one wishes high accuracy.

5. Numerical examples. For our examples, we use three boundary curves: an ellipse, the ovals of Cassini, and an "amoeba". For the ellipse, the boundary parameterization is simply

$$\mathbf{r}(s) = (a\cos s, b\sin s)\,, \qquad 0 \le s \le 2\pi \tag{55}$$

with $a, b > 0$. For the ovals of Cassini, the boundary parameterization is

$$\begin{aligned} \mathbf{r}(s) &= R(s)\,(\cos s, b\sin s) \\ R(s) &= \sqrt{\cos(2s) + \sqrt{a - \sin^2(2s)}}, \qquad 0 \le s \le 2\pi \end{aligned} \tag{56}$$

with $a > 1$, $b > 0$. The ovals of Cassini with $(a, b) = (1.1, 1)$ is shown in Figure 1. The "amoeba" boundary is defined by

$$\begin{aligned} \mathbf{r}(s) &= R(s)\,(\cos s, \sin s) \\ R(s) &= e^{\cos s}\cos^2(2s) + e^{\sin s}\sin^2(2s)\,, \qquad 0 \le s \le 2\pi \end{aligned} \tag{57}$$

and its graph is shown in Figure 2. Its interior is a decidedly nonconvex and complicated region, and we use it to illustrate that our programs can handle solutions on such unusual boundaries.

In evaluating the function $u(x, y)$, we choose a radial grid of test points. It is defined for the interior Dirichlet problem as follows.

$$\begin{aligned} \tau_j &= \frac{2j\pi}{n_\theta}, \qquad j = 0, ..., n_\theta - 1 \\ \sigma_k &= \left(\frac{k}{n_r + 1}\right)\left[2 - \frac{k}{n_r + 1}\right], \qquad k = 1, ..., n_r \\ P_{j,k} &= \sigma_k \mathbf{r}(\tau_j) \end{aligned} \tag{58}$$

along with the origin $P = (0, 0)$. The number σ_k is a measure of how close $P_{j,k}$ is to the boundary point $\mathbf{r}(\tau_j)$; and σ_k is an increasing function of k. Also, note that

$$\sigma_{n_r} = 1 - \frac{1}{(n_r + 1)^2}$$

If n_r is even moderately large, some of the points $P_{j,k}$ will be quite close to the boundary. With the Neumann method we use the slight modification

$$\begin{aligned} \tau_j &= \frac{2j\pi}{n_\theta}, \qquad j = 0, ..., n_\theta - 1 \\ \sigma_k &= \left(\frac{k}{n_r}\right)\left[2 - \frac{k}{n_r}\right], \qquad k = 1, ..., n_r \\ P_{j,k} &= \sigma_k \mathbf{r}(\tau_j) \end{aligned} \tag{59}$$

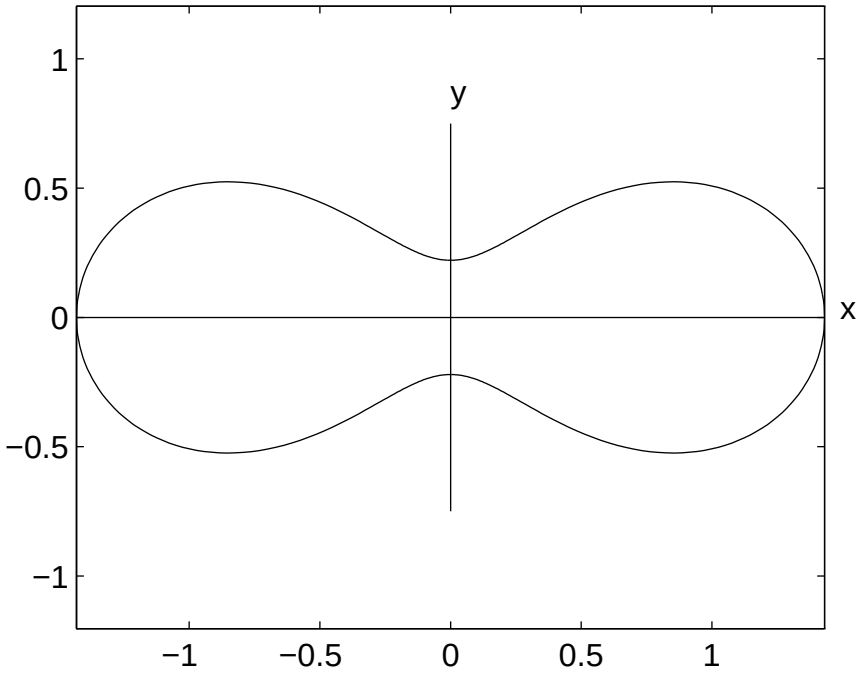

FIG. 1. *Ovals of Cassini with* $(a, b) = (1.1, 1)$

which includes points on the boundary Γ.

For exterior problems, we define σ_k and τ_j as above, and then we define

$$P_{j,k} = \frac{1}{\sigma_k}\mathbf{r}(\tau_j)$$

We also include a very distant point, to approximate a point at ∞. The test program is designed to work with any region Ω which is starlike with respect to the origin, and we have used it with regions other than those discussed here.

As test problems, we have used the following.

- Dirichlet problem:

$$\begin{aligned} \text{Interior Problem:} \quad u^{(1)} &= e^x \cos y \\ \text{Exterior Problem:} \quad u^{(2)} &= \exp\left(\frac{x}{x^2+y^2}\right)\cos\left(\frac{y}{x^2+y^2}\right) \end{aligned}$$

- Neumann problem:

$$\begin{aligned} \text{Interior Problem:} \quad u^{(3)} &= e^x \cos y - 1 \\ \text{Exterior Problem:} \quad u^{(4)} &= \frac{x}{x^2+y^2} \end{aligned}$$

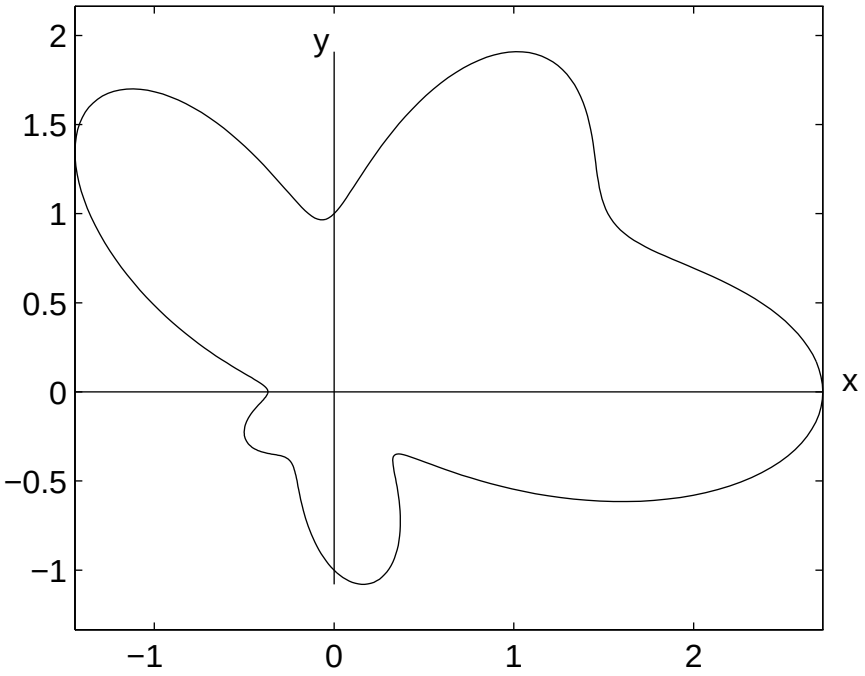

FIG. 2. *The "amoeba" boundary*

These are well-behaved functions, but they will still adequately test the procedures when combined with boundaries Γ that are more ill-behaved. We have, of course, used other test functions in addition to the ones given above. The function $u^{(2)}$ is the result of applying the Kelvin transformation (35) to $u^{(1)}$.

5.1. The Dirichlet problem. There is a great deal of data to be presented, and a combination of graphical and tabular forms seems best. We give detailed results for solving the interior Dirichlet problem for $u^{(1)}$ at the points $P_{0,k}$, $k = 0, 1, ..., n_r$ [with $P_{0,0} = (0, 0)$]. The parameter ε refers to the desired error tolerance, and n is the final order of the linear system used in INTEQN to calculate the density function ρ. The number of quadrature points used in obtaining the solution is m, and it varies with the point $P_{1,k}$.

Table 1 contains results for the ellipse with $(a, b) = (1, 5)$, with error tolerances of $\varepsilon = 10^{-3}$ and 10^{-7}. The columns labeled *Error* and *PredErr* give the actual error and the predicted error bound. *PredErr* is obtained by combining the error estimates from INTEQN and EVALU, using *EST* from (41) and the numerical integration error estimate from (49). Figure 3 gives the plots the predicted and actual errors as a function of σ_k; or more precisely, we plot

$$\{\sigma_k\} \text{ vs. } \{\log_{10} |E_k|\}, \quad k = 0, 1, ..., n_r$$

TABLE 1
Interior Dirichlet problem on an ellipse - Selected errors

	$\varepsilon = 10^{-3} \quad n = 64$				$\varepsilon = 10^{-7} \quad n = 128$		
σ_k	m	u	*Error*	*PredErr*	m	*Error*	*PredErr*
.000	128	1.0000	$-4.85E-11$	$6.99E-5$	256	$1.44E-15$	$1.62E-10$
.210	128	1.2335	$-2.51E-9$	$8.29E-5$	256	$-4.22E-15$	$4.36E-10$
.395	128	1.4845	$-1.78E-7$	$1.80E-4$	256	$-2.84E-14$	$1.99E-8$
.556	256	1.7429	$-7.21E-11$	$6.85E-5$	512	$2.89E-15$	$1.64E-10$
.691	256	1.9964	$-3.46E-8$	$8.31E-5$	512	$-5.33E-15$	$4.00E-9$
.802	256	2.2310	$-4.36E-6$	$3.14E-4$	1024	$2.22E-15$	$1.76E-10$
.889	512	2.4324	$-3.92E-7$	$1.02E-4$	1024	$-4.38E-12$	$4.37E-8$
.951	1024	2.5873	$-2.77E-7$	$8.33E-5$	2048	$-1.11E-11$	$3.10E-8$
.988	2048	2.6849	$-2.76E-6$	$9.23E-5$	8192	$-7.10E-13$	$2.09E-9$

with E_k both the predicted error and the actual error. Figure 4 gives graphs of

$$\{\sigma_k\} \text{ vs. } \{\log_{10} |u(P_{j,k}) - u_{n,m}(P_{j,k})|\}, \quad k = 0, 1, ..., n_r$$

for selected j, with $\varepsilon = 10^{-3}$. The program DRCHLT used the normal error estimates based on (43) and (50), and the grid parameters inside Ω were $n_\theta = 7$, $n_r = 8$. All computations were carried out on an HP 720 workstation. Timings are omitted, in part because they were never more than a few seconds, and in part because timings on a workstation network with many users are unreliable.

We solved the same interior Dirichlet problem, but on the "amoeba" boundary of Figure 2. When requesting an error tolerance of $\varepsilon = 10^{-4}$ and when solving at the points of (58) for $(n_\theta, n_r) = (7, 8)$, we obtained very regular behaviour in the error in the approximate values of $u^{(1)}$. The final number of nodes used in INTEQN was $n = 256$. At all points $P \in \Omega$, the predicted error bound for $u(P_{j,k}) - u_{n,m}(P_{j,k})$ was less than the requested error bound; and the actual errors were always smaller than the predicted error bound, usually much smaller.

We also solve an exterior Dirichlet problem on the elliptical region used above. In this case, the boundary $\widetilde{\Gamma}$ obtained by inverting Γ thru the unit circle is somewhat ill-behaved, as can be seen in Figure 5. The test function is $u^{(2)}$, and the other problem parameters are as before. The density function is shown in Figure 6 (with periodic extension to a larger interval), and it is clearly fairly ill-behaved around $s = 0$. The analogue of Figure 3 is given in Figure 7; and again the predicted error bound satisfies the given error tolerance. For the desired error tolerances of $\varepsilon = 10^{-3}, 10^{-7}$, the final values of n used in INTEQN were 256 and 512, respectively. The "normal" error test was used.

5.2. The Neuman problem. The principal differences in NEUMAN as compared to DRCHLT are as follows: (*i*) the error bound (27) has been changed; (*ii*) the Kelvin transform is now used to convert the interior Neumann problem to an exterior Neumann problem; and (*iii*) the potential $u(P)$ can now be evaluated at points P on the boundary

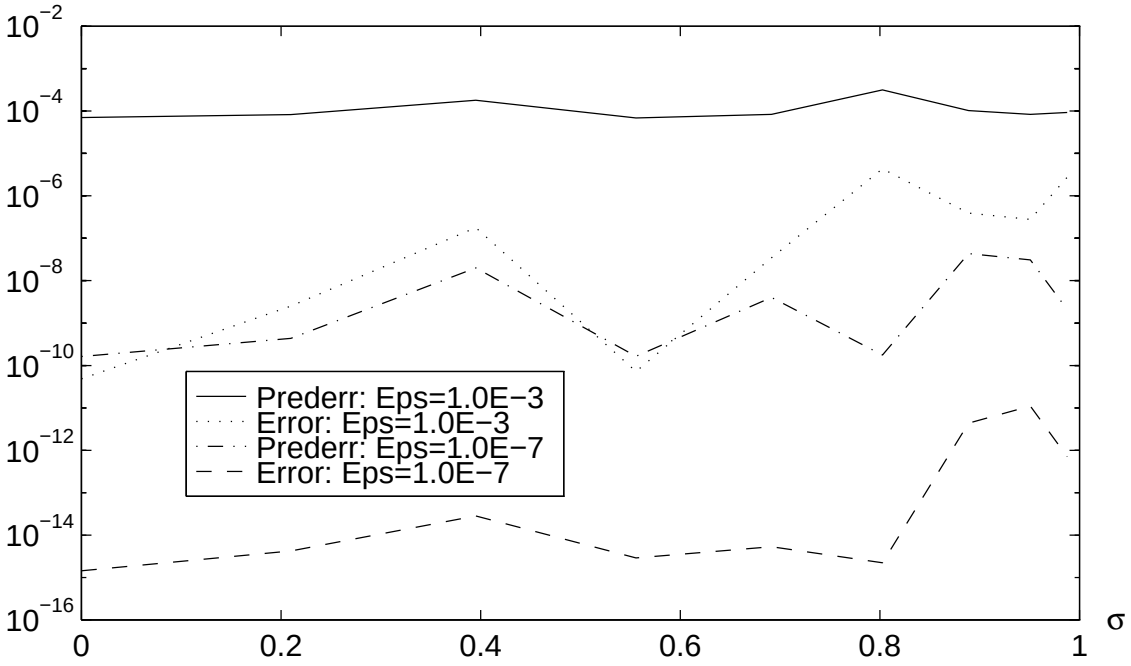

FIG. 3. *Predicted and actual errors along the radial line $\theta = 0$ for a Dirichlet problem on an ellipse*

Γ. We illustrate NEUMAN by solving the exterior Neumann problem on the ovals of Cassini shown in Figure 1, with boundary data generated from the test case $u^{(4)}$ and with error tolerances of $\varepsilon = 10^{-3}$ and 10^{-7}. The points P at which the problem is solved are given in (59), which includes boundary points on Γ; and for the parameters defining P, we used $(n_\theta, n_r) = (7, 8)$. The analogue of Figure 7, for errors along the line $\theta = 0$, is given in Figure 8; and again the predicted error bound satisfies the given error tolerance. For the desired error tolerances of $\varepsilon = 10^{-3}, 10^{-7}$, the final values of n used in INTEQN were 128 and 256, respectively.

5.3. Details on computers used in testing. The programs DRCHLT and NEUMAN were tested on several workstations and on a PC using MS Fortran 77. The workstations used were a Hewlett-Packard 720, a Hewlett-Packard C200, an SGI O2, and an IBM RS/6000. The first three used the Fortran 90 compiler delivered by the manufacturers of the machines, and the last used a Fortran 77 compiler, again supplied by the manufacturer. The examples of this paper are from the HP 720 using Fortran 90 and the default options.

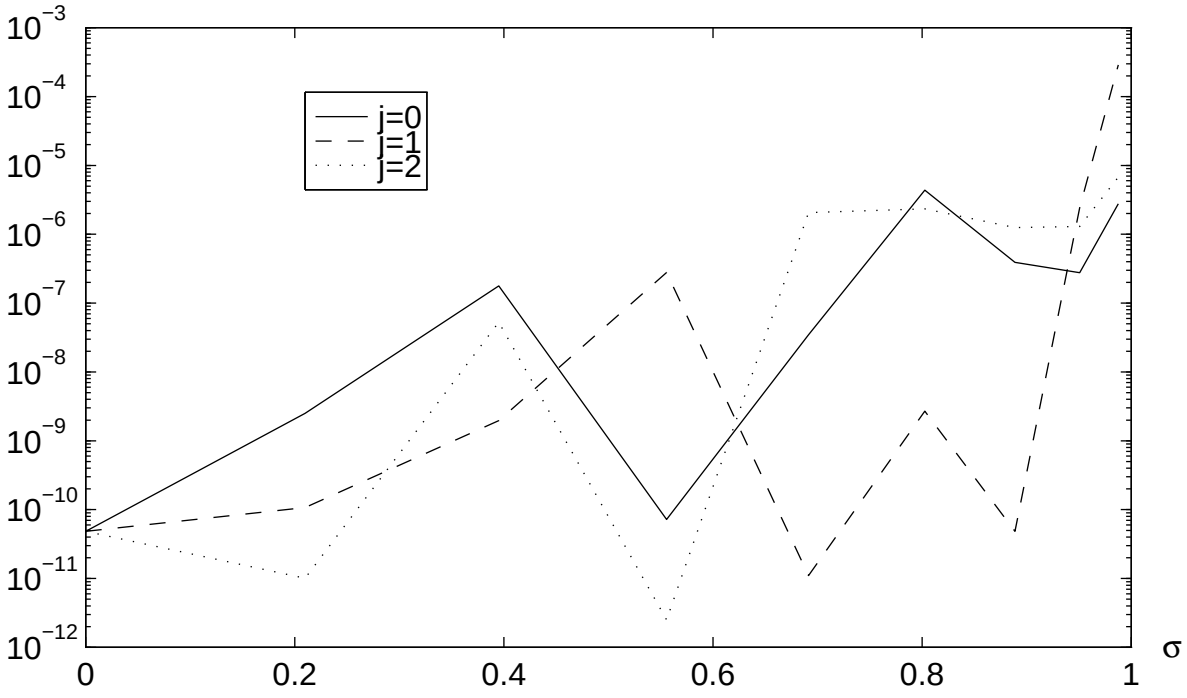

FIG. 4. *Errors along selected radial lines $\theta = \theta_j$ for a Dirichlet problem on an ellipse*

REFERENCES

[1] E. Anderson, Z. Bai, C. Bischof, J. Demmel, J. Dongarra, J. DuCroz, A. Greenbaum, S. Hammarling, A. Mckenney, S. Ostrouchov, and D. Sorenson (1992), *LAPACK Users' Guide*, SIAM Publications, Philadelphia.

[2] K. Atkinson (1976) *A Survey of Numerical Methods for the Solution of Fredholm Integral Equations of the Second Kind,* SIAM Pub.

[3] K. Atkinson (1989) *An Introduction to Numerical Analysis*, 2nd ed., John Wiley and Sons, New York.

[4] K. Atkinson (1997) *The Numerical Solution of Integral Equations of the Second Kind*, Cambridge University Press, Cambridge, UK.

[5] R. Kress (1989) *Linear Integral Equations,* Berlin, Springer.

[6] W. Mclean (1985)*Boundary Integral Equation Methods for the Laplace Equation* Ph.D thesis, Australian National University, Canberra.

[7] C. Miller (1979) *Numerical Solution of Two-Dimensional Potential Theory Problems Using Integral Equation Techniques,* Ph.D thesis, University of Iowa, Iowa City.

[8] NAG Library (1993) *D03EAF*, a program description.

[9] I. Petrovskii (1967) *Partial Differential Equations*, W. B. Saunders, Co.

[10] P. Swarztrauber (1982), Vectorizing the FFT's, in *Parallel Computations*, G. Rodrigue (editor), Academic Press, New York, pp. 51-83. (Available from the NETLIB library.)

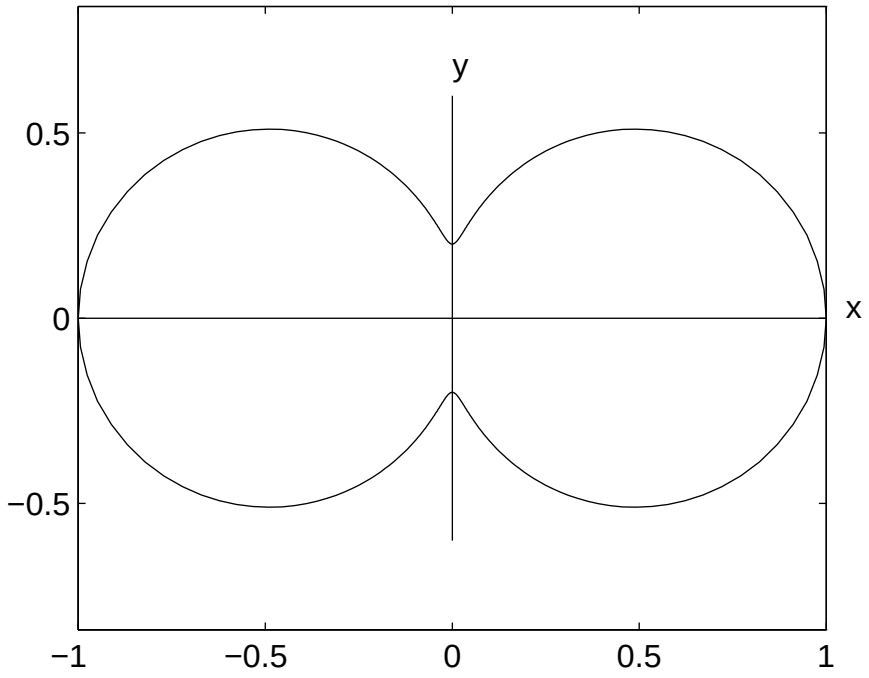

FIG. 5. *Boundary* $\widetilde{\Gamma}$ *for ellipse with* $(a, b) = (1, 5)$ *inverted thru unit circle*

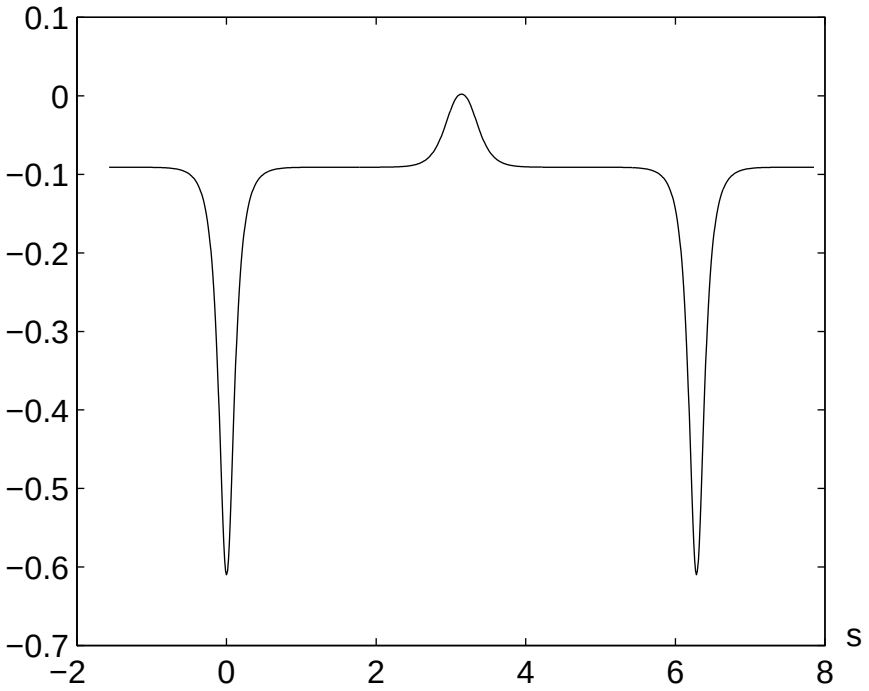

FIG. 6. *The density $\rho(s)$ on $\widetilde{\Gamma}$ for exterior Dirichlet problem defined originally outside an ellipse*

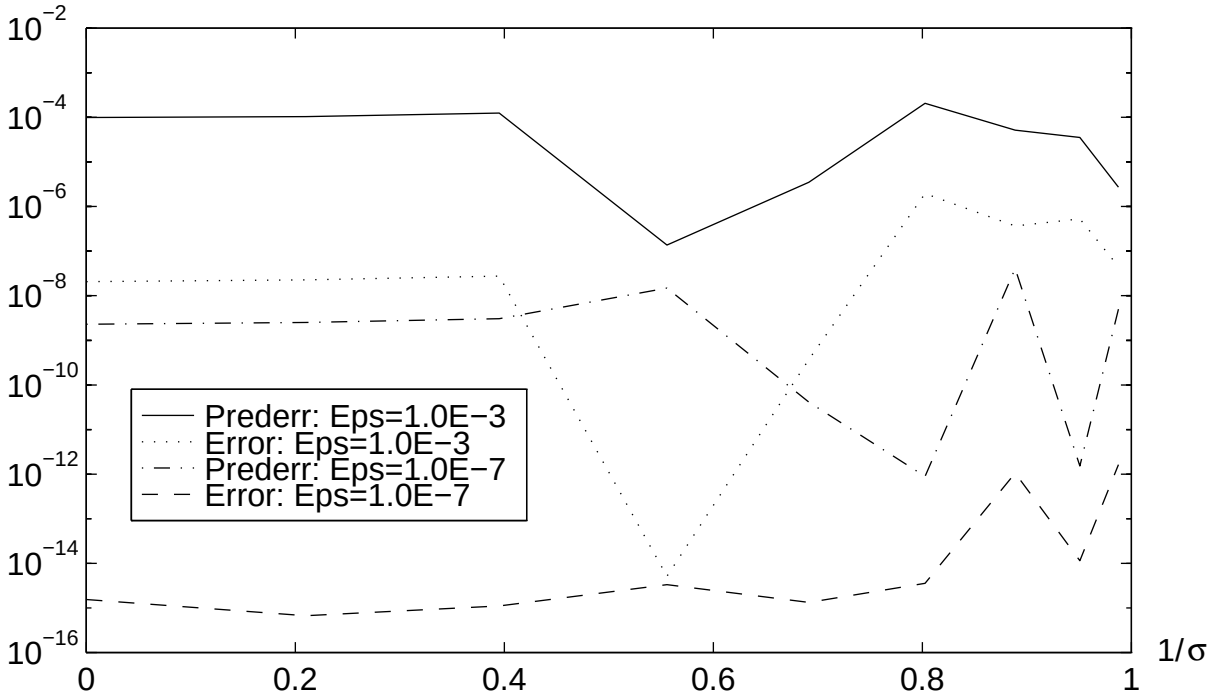

FIG. 7. *Predicted and actual errors along the radial line $\theta = 0$ for an exterior Dirichlet problem on an ellipse*

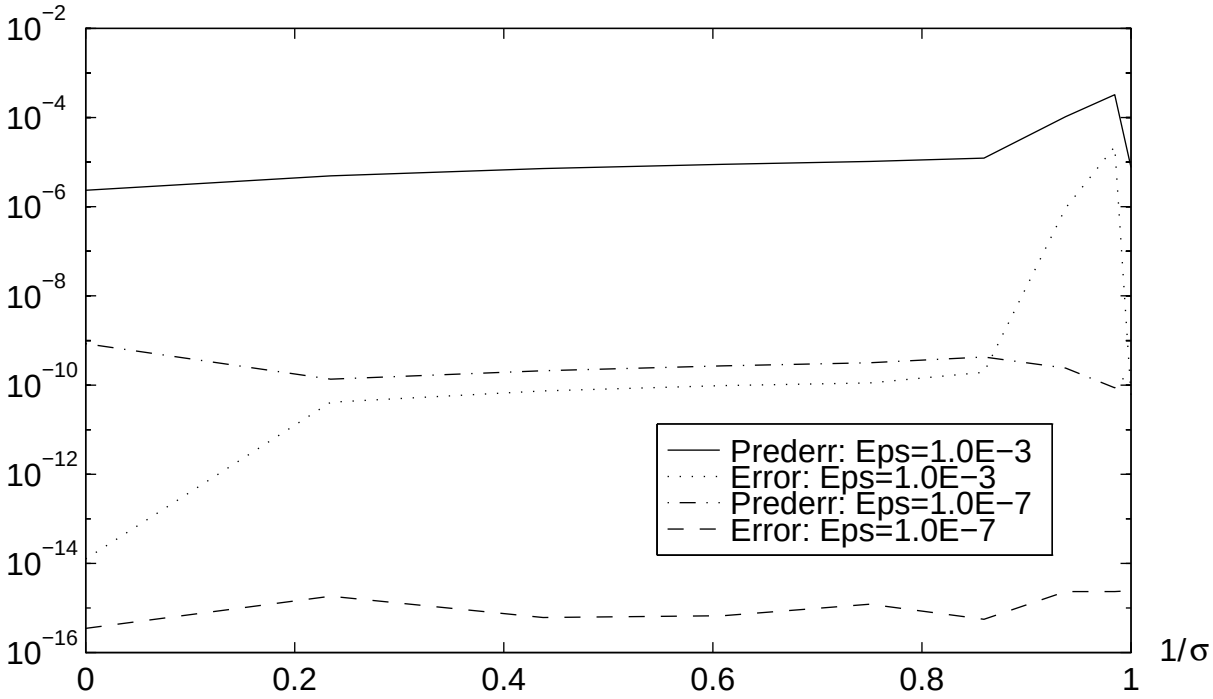

FIG. 8. *Predicted and actual errors along the radial line $\theta = 0$ for an exterior Neumann problem on an "ovals of Cassini"*